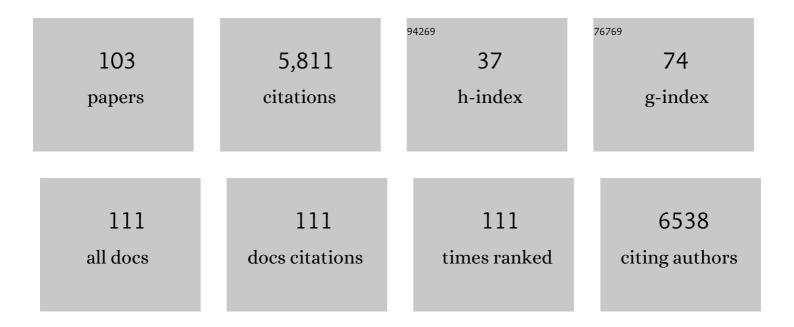
List of Publications by Year in descending order

Source: https://exaly.com/author-pdf/79301/publications.pdf Version: 2024-02-01



#	Article	IF	CITATIONS
1	Cyclophilin D deficiency attenuates mitochondrial and neuronal perturbation and ameliorates learning and memory in Alzheimer's disease. Nature Medicine, 2008, 14, 1097-1105.	15.2	833
2	Amyloid β Protein and Alzheimer's Disease: When Computer Simulations Complement Experimental Studies. Chemical Reviews, 2015, 115, 3518-3563.	23.0	530
3	The Alzheimer's Peptides Aβ40 and 42 Adopt Distinct Conformations in Water: A Combined MD / NMR Study. Journal of Molecular Biology, 2007, 368, 1448-1457.	2.0	401
4	Lysine-Specific Molecular Tweezers Are Broad-Spectrum Inhibitors of Assembly and Toxicity of Amyloid Proteins. Journal of the American Chemical Society, 2011, 133, 16958-16969.	6.6	263
5	Aβ42 is More Rigid than Aβ40 at the C Terminus: Implications for Aβ Aggregation and Toxicity. Journal of Molecular Biology, 2006, 364, 853-862.	2.0	245
6	Atomic-Level Characterization of the Ensemble of the Aβ(1–42) Monomer in Water Using Unbiased Molecular Dynamics Simulations and Spectral Algorithms. Journal of Molecular Biology, 2011, 405, 570-583.	2.0	205
7	Rational stabilization of enzymes by computational redesign of surface charge–charge interactions. Proceedings of the National Academy of Sciences of the United States of America, 2009, 106, 2601-2606.	3.3	201
8	AÎ ² Monomers Transiently Sample Oligomer and Fibril-Like Configurations: Ensemble Characterization Using a Combined MD/NMR Approach. Journal of Molecular Biology, 2013, 425, 3338-3359.	2.0	198
9	NMR R1ϕRotating-Frame Relaxation with Weak Radio Frequency Fields. Journal of the American Chemical Society, 2004, 126, 2247-2256.	6.6	151
10	Disulfide Bond Isomerization in Basic Pancreatic Trypsin Inhibitor:Â Multisite Chemical Exchange Quantified by CPMG Relaxation Dispersion and Chemical Shift Modeling. Journal of the American Chemical Society, 2003, 125, 14324-14335.	6.6	140
11	Comparison of Three Amyloid Assembly Inhibitors: The Sugar <i>scyllo-</i> Inositol, the Polyphenol Epigallocatechin Gallate, and the Molecular Tweezer CLR01. ACS Chemical Neuroscience, 2012, 3, 451-458.	1.7	109
12	Î ³ -Secretase Substrate Concentration Modulates the Aβ42/Aβ40 Ratio. Journal of Biological Chemistry, 2007, 282, 23639-23644.	1.6	101
13	The role of backbone motions in ligand binding to the c-Src SH3 domain. Journal of Molecular Biology, 2001, 313, 873-887.	2.0	91
14	Solution structure of ThiS and implications for the evolutionary roots of ubiquitin. Nature Structural Biology, 2001, 8, 47-51.	9.7	90
15	Identification of the Peptide Sequences within the EIIIA (EDA) Segment of Fibronectin That Mediate Integrin α9β1-dependent Cellular Activities. Journal of Biological Chemistry, 2008, 283, 2858-2870.	1.6	90
16	Aβ40 Protects Non-toxic Aβ42 Monomer from Aggregation. Journal of Molecular Biology, 2007, 369, 909-916.	2.0	88
17	Solution NMR Spin Relaxation Methods for Characterizing Chemical Exchange in High-Molecular-Weight Systems. Methods in Enzymology, 2005, 394, 430-465.	0.4	86
18	Characterization of AÎ ² Monomers through the Convergence of Ensemble Properties among Simulations with Multiple Force Fields. Journal of Physical Chemistry B, 2016, 120, 259-277.	1.2	81

#	Article	IF	CITATIONS
19	Mapping Chemical Exchange in Proteins with MW > 50 kD. Journal of the American Chemical Society, 2003, 125, 8968-8969.	6.6	77
20	EGCG binds intrinsically disordered N-terminal domain of p53 and disrupts p53-MDM2 interaction. Nature Communications, 2021, 12, 986.	5.8	77
21	An improved method for distinguishing between anisotropic tumbling and chemical exchange in analysis of 15N relaxation parameters. Journal of Biomolecular NMR, 2001, 20, 149-165.	1.6	73
22	Targeting Amyloidogenic Processing of APP in Alzheimer's Disease. Frontiers in Molecular Neuroscience, 2020, 13, 137.	1.4	73
23	Familial Alzheimer's mutations within APPTM increase Aβ42 production by enhancing accessibility of ε-cleavage site. Nature Communications, 2014, 5, 3037.	5.8	72
24	3â€ <i>O</i> â€Sulfation of Heparan Sulfate Enhances Tau Interaction and Cellular Uptake. Angewandte Chemie - International Edition, 2020, 59, 1818-1827.	7.2	71
25	Solution NMR and Computer Simulation Studies of Active Site Loop Motion in Triosephosphate Isomeraseâ€. Biochemistry, 2006, 45, 10787-10794.	1.2	70
26	CPMG sequences with enhanced sensitivity to chemical exchange. Journal of Biomolecular NMR, 2001, 21, 361-366.	1.6	69
27	Dynamics of ATP-binding Cassette Contribute to Allosteric Control, Nucleotide Binding and Energy Transduction in ABC Transporters. Journal of Molecular Biology, 2004, 342, 525-537.	2.0	69
28	Glycan Determinants of Heparin-Tau Interaction. Biophysical Journal, 2017, 112, 921-932.	0.2	68
29	Surface Plasmon Resonance and Nuclear Magnetic Resonance Studies of ABADâ^'Aβ Interaction. Biochemistry, 2007, 46, 1724-1731.	1.2	67
30	Ligand-Induced Strain in Hydrogen Bonds of the c-Src SH3 Domain Detected by NMR. Journal of Molecular Biology, 2000, 304, 497-505.	2.0	66
31	M35 Oxidation Induces Al²40-like Structural and Dynamical Changes in Al²42. Journal of the American Chemical Society, 2008, 130, 5394-5395.	6.6	64
32	Highly Conserved Histidine Plays a Dual Catalytic Role in Protein Splicing: A p <i>K</i> _a Shift Mechanism. Journal of the American Chemical Society, 2009, 131, 11581-11589.	6.6	62
33	Solution NMR methods for quantitative identification of chemical exchange in15N-labeled proteins. Magnetic Resonance in Chemistry, 2003, 41, 866-876.	1.1	54
34	p <i>K</i> _a Coupling at the Intein Active Site: Implications for the Coordination Mechanism of Protein Splicing with a Conserved Aspartate. Journal of the American Chemical Society, 2011, 133, 10275-10282.	6.6	45
35	Molecular Tweezers Inhibit Islet Amyloid Polypeptide Assembly and Toxicity by a New Mechanism. ACS Chemical Biology, 2015, 10, 1555-1569.	1.6	45
36	Intramolecular Disulfide Bond between Catalytic Cysteines in an Intein Precursor. Journal of the American Chemical Society, 2012, 134, 2500-2503.	6.6	44

#	Article	IF	CITATIONS
37	Vitamin B12 modulates Parkinson's disease LRRK2 kinase activity through allosteric regulation and confers neuroprotection. Cell Research, 2019, 29, 313-329.	5.7	42
38	Drug delivery of memantine with carbon dots for Alzheimer's disease: blood–brain barrier penetration and inhibition of tau aggregation. Journal of Colloid and Interface Science, 2022, 617, 20-31.	5.0	35
39	C-Terminal Tetrapeptides Inhibit Aβ42-Induced Neurotoxicity Primarily through Specific Interaction at the N-Terminus of Aβ42. Journal of Medicinal Chemistry, 2011, 54, 8451-8460.	2.9	34
40	Major Differences between the Self-Assembly and Seeding Behavior of Heparin-Induced and in Vitro Phosphorylated Tau and Their Modulation by Potential Inhibitors. ACS Chemical Biology, 2019, 14, 1363-1379.	1.6	34
41	Selection and Structure of Hyperactive Inteins: Peripheral Changes Relayed to the Catalytic Center. Journal of Molecular Biology, 2009, 393, 1106-1117.	2.0	33
42	Methyl dynamics of the amyloid-β peptides Aβ40 and Aβ42. Biochemical and Biophysical Research Communications, 2007, 362, 410-414.	1.0	31
43	Internal Disulfide Bond Acts as a Switch for Intein Activity. Biochemistry, 2013, 52, 5920-5927.	1.2	30
44	Differential multiple quantum relaxation caused by chemical exchange outside the fast exchange limit. Journal of Biomolecular NMR, 2002, 24, 263-268.	1.6	29
45	Structural and Mutational Studies of a Hyperthermophilic Intein from DNA Polymerase II of Pyrococcus abyssi. Journal of Biological Chemistry, 2011, 286, 38638-38648.	1.6	27
46	Metal ions binding to recA inteins from Mycobacterium tuberculosis. Molecular BioSystems, 2009, 5, 644.	2.9	24
47	Backbone Dynamics and Global Effects of an Activating Mutation in Minimized Mtu RecA Inteins. Journal of Molecular Biology, 2010, 400, 755-767.	2.0	23
48	Structure-activity relationship of carbon nitride dots in inhibiting Tau aggregation. Carbon, 2022, 193, 1-16.	5.4	20
49	Mutual synergistic protein folding in split intein. Bioscience Reports, 2012, 32, 433-442.	1.1	19
50	A Single Aspartate Coordinates Two Catalytic Steps in Hedgehog Autoprocessing. Journal of the American Chemical Society, 2016, 138, 10806-10809.	6.6	17
51	Hedgehog Cholesterolysis: Specialized Gatekeeper to Oncogenic Signaling. Cancers, 2015, 7, 2037-2053.	1.7	17
52	Active Site Targeting of Hedgehog Precursor Protein with Phenylarsine Oxide. ChemBioChem, 2015, 16, 55-58.	1.3	16
53	The Sulfation Code of Tauopathies: Heparan Sulfate Proteoglycans in the Prion Like Spread of Tau Pathology. Frontiers in Molecular Biosciences, 2021, 8, 671458.	1.6	16
54	Zinc Inhibits Hedgehog Autoprocessing. Journal of Biological Chemistry, 2015, 290, 11591-11600.	1.6	15

#	Article	IF	CITATIONS
55	Structural analysis of a glucoglucuronan derived from laminarin and the mechanisms of its anti-lung cancer activity. International Journal of Biological Macromolecules, 2020, 163, 776-787.	3.6	15
56	Inhibition of Staphylococcus aureus biofilm-forming functional amyloid by molecular tweezers. Cell Chemical Biology, 2021, 28, 1310-1320.e5.	2.5	15
57	Coupled Transmembrane Substrate Docking and Helical Unwinding in Intramembrane Proteolysis of Amyloid Precursor Protein. Scientific Reports, 2018, 8, 12411.	1.6	14
58	Protein–Nucleic Acid Conjugation with Sterol Linkers Using Hedgehog Autoprocessing. Bioconjugate Chemistry, 2019, 30, 2799-2804.	1.8	13
59	1H, 13C, and 15N NMR assignments of an engineered intein based on Mycobacterium tuberculosis RecA. Biomolecular NMR Assignments, 2008, 2, 111-113.	0.4	12
60	Protection Mechanisms Against Aβ42 Aggregation. Current Alzheimer Research, 2008, 5, 548-554.	0.7	12
61	Subverting Hedgehog Protein Autoprocessing by Chemical Induction of Paracatalysis. Biochemistry, 2020, 59, 736-741.	1.2	12
62	Tranilast Binds to Al ² Monomers and Promotes Al ² Fibrillation. Biochemistry, 2013, 52, 3995-4002.	1.2	11
63	Intrinsically Disordered N-terminal Domain (NTD) of p53 Interacts with Mitochondrial PTP Regulator Cyclophilin D. Journal of Molecular Biology, 2022, 434, 167552.	2.0	11
64	Homogalacturonan from squash: Characterization and tau-binding pattern of a sulfated derivative. Carbohydrate Polymers, 2022, 285, 119250.	5.1	11
65	Intein-Promoted Cyclization of Aspartic Acid Flanking the Intein Leads to Atypical N-Terminal Cleavage. Biochemistry, 2017, 56, 1042-1050.	1.2	10
66	Sterol A-ring plasticity in hedgehog protein cholesterolysis supports a primitive substrate selectivity mechanism. Chemical Communications, 2019, 55, 1829-1832.	2.2	10
67	Coil-to-α-helix transition at the Nup358-BicD2 interface activates BicD2 for dynein recruitment. ELife, 2022, 11, .	2.8	10
68	Expression, purification, and reconstitution of the transmembrane domain of the human amyloid precursor protein for NMR studies. Protein Expression and Purification, 2012, 81, 11-17.	0.6	9
69	V67L Mutation Fills an Internal Cavity To Stabilize RecA <i>Mtu</i> Intein. Biochemistry, 2017, 56, 2715-2722.	1.2	9
70	Interactions of fibroblast growth factors with sulfated galactofucan from Saccharina japonica. International Journal of Biological Macromolecules, 2020, 160, 26-34.	3.6	9
71	Solution NMR Studies of Aβ Monomer Dynamics. Protein and Peptide Letters, 2011, 18, 354-361.	0.4	8
72	Effects of Alzheimer's Disease-Related Proteins on the Chirality of Brain Endothelial Cells. Cellular and Molecular Bioengineering, 2021, 14, 231-240.	1.0	8

#	Article	IF	CITATIONS
73	Synthesis of 3- <i>O</i> -Sulfated Heparan Sulfate Oligosaccharides Using 3- <i>O</i> -Sulfotransferase Isoform 4. ACS Chemical Biology, 2021, 16, 2026-2035.	1.6	8
74	1H, 13C, and 15N NMR assignments of a Drosophila Hedgehog autoprocessing domain. Biomolecular NMR Assignments, 2014, 8, 279-281.	0.4	7
75	pH-dependent and dynamic interactions of cystatin C with heparan sulfate. Communications Biology, 2021, 4, 198.	2.0	7
76	High pressure NMR reveals conformational perturbations by disease-causing mutations in amyloid β-peptide. Chemical Communications, 2018, 54, 4609-4612.	2.2	6
77	General Base Swap Preserves Activity and Expands Substrate Tolerance in Hedgehog Autoprocessing. Journal of the American Chemical Society, 2019, 141, 18380-18384.	6.6	6
78	High-resolution crystal structures of two crystal forms of human cyclophilin D in complex with PEG 400 molecules. Acta Crystallographica Section F, Structural Biology Communications, 2014, 70, 717-722.	0.4	5
79	Intein Inhibitors as Novel Antimicrobials: Protein Splicing in Human Pathogens, Screening Methods, and Off-Target Considerations. Frontiers in Molecular Biosciences, 2021, 8, 752824.	1.6	5
80	Nanomolar, Noncovalent Antagonism of Hedgehog Cholesterolysis: Exception to the "Irreversibility Rule―for Protein Autoprocessing Inhibition. Biochemistry, 2022, 61, 1022-1028.	1.2	5
81	1H, 15N and 13C backbone assignment of MJ1267, an ATP-binding cassette. Journal of Biomolecular NMR, 2002, 24, 167-168.	1.6	4
82	Characterization of Heparin's Conformational Ensemble by Molecular Dynamics Simulations and Nuclear Magnetic Resonance Spectroscopy. Journal of Chemical Theory and Computation, 2022, 18, 1894-1904.	2.3	4
83	1H, 13C, and 15N NMR assignments of the Pyrococcus abyssi DNA polymerase II intein. Biomolecular NMR Assignments, 2011, 5, 233-235.	0.4	3
84	Substrate–Enzyme Interactions in Intramembrane Proteolysis: γ-Secretase as the Prototype. Frontiers in Molecular Neuroscience, 2020, 13, 65.	1.4	3
85	Substrate interaction inhibits γ-secretase production of amyloid-β peptides. Chemical Communications, 2020, 56, 2578-2581.	2.2	3
86	Hedgehog Autoprocessing: From Structural Mechanisms to Drug Discovery. Frontiers in Molecular Biosciences, 2022, 9, .	1.6	3
87	Solution NMR and Computer Simulation Studies of Active Site Loop Motion in Triosephosphate Isomerase. Biochemistry, 2006, 45, 14232-14232.	1.2	2
88	3―O â€Sulfation of Heparan Sulfate Enhances Tau Interaction and Cellular Uptake. Angewandte Chemie, 2020, 132, 1834-1843.	1.6	2
89	Characterization of the Structural Ensembles of AÎ ² Monomers using a Combined MD/NMR Approach. Biophysical Journal, 2012, 102, 631a-632a.	0.2	1
90	Coordination of the third step of protein splicing in two cyanobacterial inteins. FEBS Letters, 2017, 591, 2147-2154.	1.3	1

#	Article	IF	CITATIONS
91	Allosteric Influence of Extremophile Hairpin Motif Mutations on the Protein Splicing Activity of a Hyperthermophilic Intein. Biochemistry, 2020, 59, 2459-2467.	1.2	1
92	An alternative domain-swapped structure of the Pyrococcus horikoshii Polll mini-intein. Scientific Reports, 2021, 11, 11680.	1.6	1
93	Aß Monomers Transiently Sample Oligomer and Fibril-Like Configurations: Ensemble Characterization using a Combined MD/NMR Approach. Biophysical Journal, 2013, 104, 56a.	0.2	0
94	Systematic Characterization of Wild Type and Familial Alzheimer's Disease Mutant Aβ Monomers Through the Convergence of Ensembles Simulated with Different Force Fields. Biophysical Journal, 2014, 106, 269a.	0.2	0
95	Zinc Inhibits Hedgehog Autoprocessing: Linking Zinc Deficiency with Hedgehog Activation. Biophysical Journal, 2015, 108, 531a.	0.2	0
96	P4â€521: 3â€Oâ€SULFO GROUP IS A KEY DETERMINANT IN TAUâ€GLYCAN INTERACTION. Alzheimer's and Demer 2019, 15, P1514.	ntia. 0.4	0
97	F2â€06â€01: MAJOR DIFFERENCES BETWEEN THE SELFâ€ASSEMBLY, SEEDING BEHAVIOR, AND INTERACTION WI MODULATORS OF HEPARINâ€INDUCED VERSUS INâ€VITRO PHOSPHORYLATED TAU. Alzheimer's and Dementia, 2019, 15, P524.		0
98	P4â€687: SUBSTRATE BINDING INHIBITS γâ€SECRETASE CLEAVAGE OF AMYLOID PRECURSOR PROTEIN. Alzheimo and Dementia, 2019, 15, .	er's 0.4	0
99	In Vitro Effects of (+)MK-801 (dizocilpine) and Memantine on β-Amyloid Peptides Linked to Alzheimer's Disease. Biochemistry, 2020, 59, 4517-4522.	1.2	0
100	Frontispiz: 3â€≺i>Oâ€Sulfation of Heparan Sulfate Enhances Tau Interaction and Cellular Uptake. Angewandte Chemie, 2020, 132, .	1.6	0
101	Frontispiece: 3â€∢i>Oâ€Sulfation of Heparan Sulfate Enhances Tau Interaction and Cellular Uptake. Angewandte Chemie - International Edition, 2020, 59, .	7.2	0
102	Methods to Study the Structure and Catalytic Activity of cis-Splicing Inteins. Methods in Molecular Biology, 2020, 2133, 55-73.	0.4	0
103	Discovery of the first tightâ€binding reversible antagonists of Hedgehog protein autoprocessing. FASEB Journal, 2022, 36, .	0.2	0